Optical Pulse and Beam Propagation II
Volume 3927

PROCEEDINGS OF SPIE
SPIE—The International Society for Optical Engineering

Optical Pulse and Beam Propagation II

Yehuda B. Band
Chair/Editor

25–27 January 2000
San Jose, California

Sponsored by
AFOSR—U.S. Air Force Office of Scientific Research
SPIE—The International Society for Optical Engineering

Published by
SPIE—The International Society for Optical Engineering

Volume 3927

The papers appearing in this book compose the proceedings of the technical conference cited on the cover and title page of this volume. They reflect the authors' opinions and are published as presented, in the interests of timely dissemination. Their inclusion in this publication does not necessarily constitute endorsement by the editors or by SPIE. Papers were selected by the conference program committee to be presented in oral or poster format, and were subject to review by volume editors or program committees.

Please use the following format to cite material from this book:

Author(s), "Title of paper," in *Optical Pulse and Beam Propagation II*, Yehuda B. Band, Editor, Proceedings of SPIE Vol. 3927, page numbers (2000).

ISSN 0277-786X
ISBN 0-8194-3544-9

Published by
SPIE—The International Society for Optical Engineering
P.O. Box 10, Bellingham, Washington 98227-0010 USA
Telephone 360/676-3290 (Pacific Time) • Fax 360/647-1445

Printed in the United States of America.

Contents

Conference Committee

Conference Chair

Yehuda B. Band, Ben-Gurion University of the Negev (Israel)

Program Committee

Akira Hasegawa, Kochi University of Technology (Japan) and NTT Science and Core Technology Laboratory (Japan)
Gordon S. Kino, Stanford University
Norman S. Kopeika, Ben-Gurion University of the Negev (Israel)
Jerzy S. Krasinski, Oklahoma State University

Session Chairs

1 Fiber
Akira Hasegawa, Kochi University of Technology (Japan) and NTT Science and Core Technology Laboratory (Japan)

2 Nonlinear
Jerzy S. Krasinski, Oklahoma State University

3A Beam Propagation in Random Media I
Norman S. Kopeika, Ben-Gurion University of the Negev (Israel)

3B Beam Propagation in Random Media II
Steven L. Jacques, Oregon Medical Laser Center

3C Beam Propagation in Random Media III
Steven L. Jacques, Oregon Medical Laser Center

3D Beam Propagation in Random Media IV
Norman S. Kopeika, Ben-Gurion University of the Negev (Israel)

SESSION 1

Fiber

Invited Paper

Bragg Soliton Polarization Evolution

R. E. Slusher[a], Suresh Pereira[b], Stefan Spälter[a], B. J. Eggleton[a], and J. E. Sipe[b]

[a]Lucent Technologies,
700 Mountain Avenue, Murray Hill, NJ 07974 USA

[b]Department of Physics, University of Toronto,
Ontario, Canada M5S1A7

ABSTRACT

Nonlinear propagation of optical pulses in fiber Bragg gratings is studied experimentally and with numerical simulations of the coupled mode equations. After a review of enhanced nonlinear interactions for pulse wavelengths near the short wavelength edge of the photonic bandgap associated with the grating, this study explores polarization evolution during nonlinear pulse propagation. Initial results for polarization instabilities and expectations for vector Bragg solitons are described.

Keywords: fiber gratings, solitons, birefringence, polarization instability

1. BRAGG SOLITONS

Many of the nonlinear optical pulse propagation phenomena observed in standard optical fiber, including solitons[1] and polarization instabilities[2-4], can also be found in fiber gratings. However, the fiber grating allows strong variation in the propagation parameters over a limited span of wavelengths near the one-dimensional photonic bandgap formed by the grating resulting in nonlinear pulse evolution in much shorter distances than in normal fiber.

The photonic bandgap for the fiber gratings used in the experiments described in this paper is shown in Figure 1. The transmission through the fiber grating goes nearly to zero within the photonic bandgap that extends over approximately 0.17 nm in wavelength, corresponding to an index modulation for the grating of $\Delta n = 2x10^{-4}$. We will focus our attention on wavelengths outside the bandgap near the short wavelength gap edge. There are actually two bandgaps seen in Figure 1 corresponding to input polarizations along the fast and slow principle polarization axes. The birefringence of the grating is

$$\Delta n_{br} = n_y - n_x \tag{1}$$

where n_x and n_y are the indices along the fast and slow polarization axes respectively. For the grating used in our experiments $\Delta n_{br} = 3.6x10^{-5}$.

Examples of the parameters that can be varied by tuning the wavelength of the optical pulse relative to the photonic bandgap are the group velocity,

$$v_g = v(f^2-1)^{1/2}/f \tag{2}$$

where v is the pulse velocity in the fiber with no grating and f is the detuning from the edge of the photonic bandgap in units of half-gap measured from the center of the fast axis gap, and the dispersion

$$\beta_2 = [(1-(v_g/v)^2)/(v_g/v)^3]/v^2fK \tag{3}$$

where $K = \pi \Delta n/\lambda_o$ is the half bandgap in units of cm^{-1} and λ_o is the free space wavelength. Note that v_g goes to zero at the gap edge. The dispersion near the gap can be nearly 10^5 higher than in normal fiber. This means that optical solitons can be

Correspondence: R. E. Slusher. Other author information: R. E. S.: Email: res@bell-labs.com; Telephone: (908)582-4094; Fax: (908)582-3260.

In *Optical Pulse and Beam Propagation II*, Yehuda B. Band, Editor,
Proceedings of SPIE Vol. 3927 (2000) • 0277-786X/00/$15.00

formed in a few centimeters instead of hundreds of meters required for normal fiber. Of course, very high optical intensities are required in order to compensate the large dispersion with nonlinear interactions in such short distances. However we have shown previously that the effective nonlinearity is also enhanced by a factor

$$F_{nl} = (3 - (v_g/v)^2) / 2(v_g/v)^2 \quad (4)$$

This nonlinear enhancement is typically a factor near two for detuning near the gap. The amount of enhancement is limited by the spread of frequencies in the optical pulse. When these frequency components approach the gap, they begin to be reflected from the grating and the intensity propagating through the grating is reduced. We minimize these reflection effects in our experiments by using an apodized grating. The effective birefringence can also increase for wavelengths near the gap. This increase is associated with the increased interaction time as the group velocity decreases.

We have shown[1] that, even though the dispersion is changing rapidly near the gap, one can approximate the pulse dynamics with a nonlinear Schröedinger equation where the nonlinear interaction and dispersion are enhanced by the factors show in Eqs. (3) and (4). We have previously demonstrated propagating solitons experimentally[1]. This paper extends the

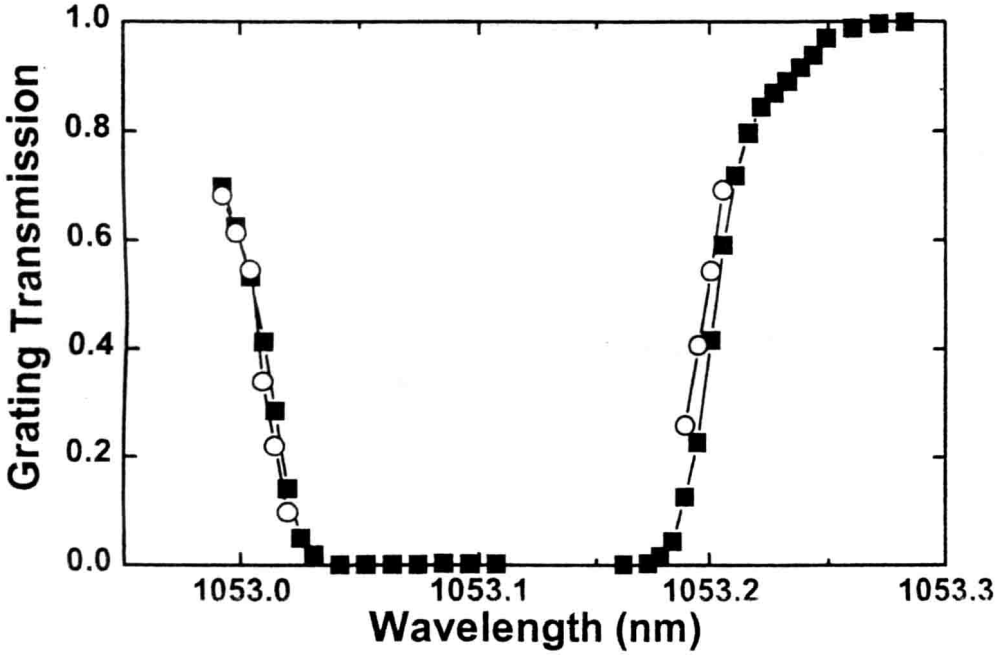

Figure 1 The transmission of the fiber grating is shown for the fast X axis (open circles) and the slow Y axis (solid squares). The difference in the band-gaps is predominately at the long wavelength edge and corresponds to a birefringence of 3.6×10^{-6}. The resolution is limited by the optical pulse width of 0.03nm. The small difference in gap widths at the long wavelength edge was very reproducible in spite of the limiting resolution.

nonlinear pulse propagation study to include polarization effects that result from the grating birefringence. We can approximate the dynamics of the system using a set of two, coupled nonlinear Schröedinger equations[5],

$$i(\partial/\partial t + \omega'_x \partial/\partial z)X + 1/2\ \omega_x'' \partial^2 X/\partial z^2 + \{\alpha^x_{spm}|X|^2 + \alpha^x_{cpm}|Y|^2\}X + \alpha^x_{pc} Y^2 X^* e^{i\sigma t} = 0 \quad (5)$$

$$i(\partial/\partial t + \omega'_y \partial/\partial z)Y + 1/2\ \omega_y'' \partial^2 Y/\partial z^2 + \{\alpha^y_{spm}|Y|^2 + \alpha^y_{cpm}|X|^2\}X + \alpha^y_{pc} X^2 Y^* e^{-i\sigma t} = 0 \quad (6)$$

where X and Y are the polarized field components along the principal polarization axes, $\sigma = 2(k_x - k_y)$ is the wave-vector mismatch between the two polarizations, z is the propagation direction and the α coefficients corresponding to self phase modulation (spm), cross phase modulation (cpm), and phase conjugation (pc) are in the ratio $\alpha^x_{spm}:\alpha^x_{cpm}:\alpha^x_{pc} = 3:2:1$. The polarization fields are centered around the frequencies ω_x and ω_y whose numerical values are equal, but whose derivatives (with respect to the corresponding wave-vectors) representing the group velocity and dispersion, will be unequal due to birefringence. Furthermore, the wave-vectors, k_x and k_y, associated with the polarization fields will be different due to birefringence. Energy exchange between the two polarization components proceeds via the last term in both equations. A more rigorous set of four coupled equations[5] is used for numerical simulations that model our experiments.

2. EXPERIMENTAL APPARATUS

The experimental arrangement is shown in Figure 2. The pulsed light source is a Q-switched mode-locked YLF laser that produces 80ps wide pulses at 1053nm wavelengths [1]. The center position of the bandgap is tuned with respect to the laser wavelength by straining the fiber. The frequency components of the optical pulse are primarily outside the photonic bandgap in contrast to recent nonlinear polarization switching experiments [6]. A fast detector and sampling oscilloscope resolve the pulse shapes. An energy meter measures the incident pulse energies. The pulse spectral width, near 0.03nm, limits the resolution of the data shown in Figure 1.

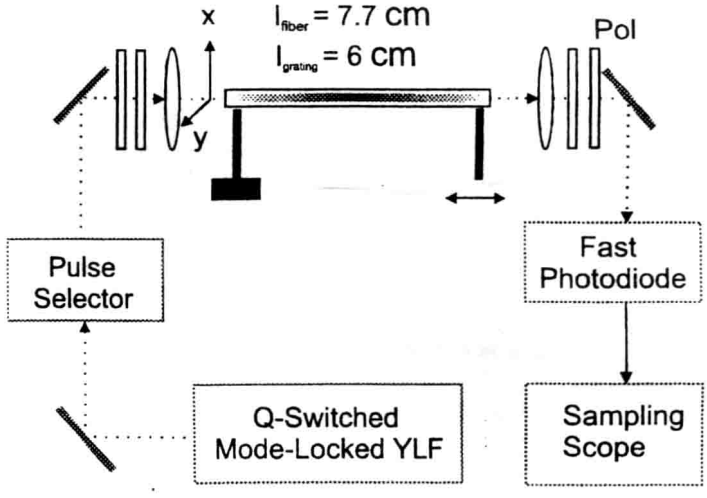

Figure 2 Schematic diagram of the experimental apparatus

The input polarization state of the optical pulse is set by the combined orientations of a half-wave and quarter-wave plate immediately before the input focusing lens. The measured output polarization is selected using a half-wave plate and a linear polarizer after the fiber grating.

The fiber grating has an overall length of 7.7 cm with 0.75 cm apodized sections at both ends. This apodization eliminates reflection for wavelengths near the gap edge as seen in Figure 1. The average grating index is very nearly constant throughout the entire fiber. The fiber ends are cleaved so that there is less than 1 mm of normal fiber at each end in order to simplify the

analysis of the nonlinear interactions. The grating birefringence is much larger than the normal fiber birefringence due to the UV grating writing process. We find, that in addition to offset X and Y gaps, that fast X gap is 3% smaller than the slow Y gap. This results in a near alignment of the short wavelength X and Y gap edges. This further simplifies our experimental analysis since the fast and slow polarization pulse components are nearly equally reflected from the gap edge and experience nearly equal dispersion and nonlinear enhancements (see Eqs. (2) and (3)). The near coincidence of the short wavelength bandgaps results in a nearly constant effective birefringence as the pulse wavelengths approach the gap.

Linear pulse propagation measurements are made using peak pulse intensities less than 0.5 GW/cm^2 where nonlinear effects are negligible. The intensities used in the nonlinear experiments were limited to less than 10 GW/cm^2 in order to avoid damaging the grating.

3. POLARIZATION EVOLUTION

Polarized pulse experiments are complex since the polarization state evolves throughout the pulse for both the linear and nonlinear pulse intensity regimes. Both the ellipticity and the angular orientation of the polarization ellipse vary during the pulse. In principle the Stokes vector can be measured during the pulse, but this requires six different settings of the measured polarization states. The measurements reported here were made only along the principle polarization axes. The complex pulse polarization states do allow a good determination of the polarization properties of the grating. We fit our linear experimental pulse shapes with numerically modeled shapes in order to determine the grating birefringence at both the long and short wavelength edges of the grating. These measurements yield a birefringence of 3.6×10^{-6}, which is consistent with the results shown in Figure 1.

At peak pulse intensities above 5 GW/cm^2 the nonlinear index change, $n_2 I$, where $n_2 = 2.6 \times 10^{-16}$ cm^2/W is the nonlinear index of refraction for silica and I is the peak pulse intensity, becomes comparable with the birefringence. At these intensities we expect a polarization instability[2,3]. The instability results in a transfer of energy from the fast polarization component to the slow component. The terms responsible for the energy exchange in the nonlinear Schröedinger equations can be seen as the

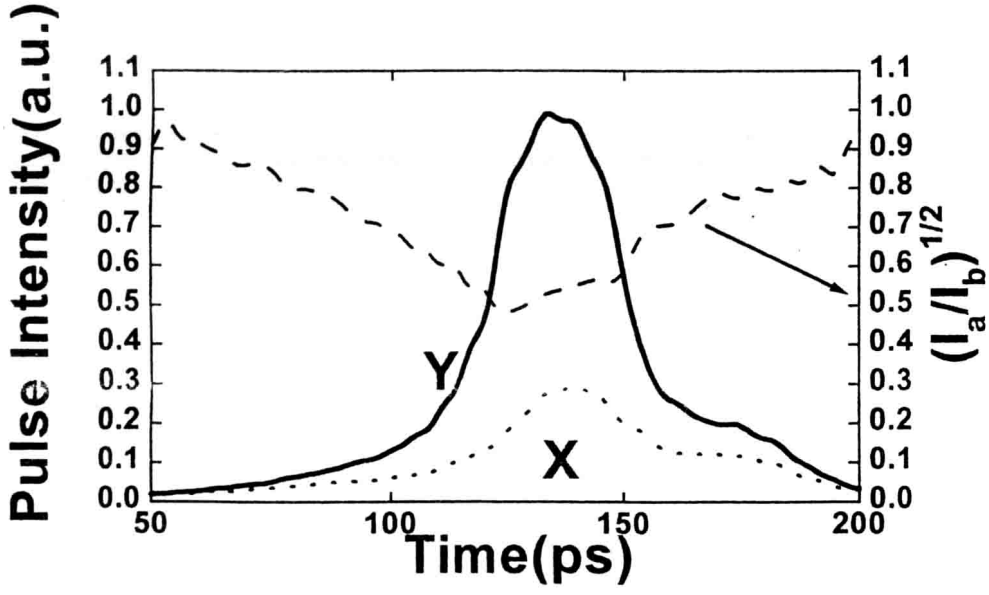

Figure 3 Pulse shapes for the X (dotted) and Y (solid) polarization components after transmission through the fiber grating with equal input peak intensities of 4 GW/cm^2 in each polarization component. The square root of the intensity ratio, the ellipticity is shown as a dashed curve with the scale on the right axis.

last terms in Eqs (5) and (6). An example of the instability observed experimentally for our fiber grating is shown in Figure 3. The input X and Y components are both equal at 4 GW/cm^2 in this example. Note that there is a clear transfer of energy to the slow Y component after propagating through the grating. The ratio of the pulse amplitudes along the major and minor axes of the polarization ellipse, i.e. the ellipticity, shown as a dashed curve in Figure 3, illustrates the evolution of the polarization state during the pulse.

The polarization instability is most dramatic for input polarizations aligned nearly along the fast axis. If the input polarization is aligned near the slow axis, it only rotates slightly further toward the slow axis. These effects are shown in Figure 4 for the two extreme alignment cases. Note the strong conversion from the fast axis to the slow axis in comparing Figure 4 (a) and (c), while there is little change in the angular orientation of the polarization in (b) and (d) where the input polarization is near the slow axis. The detuning in Figure 4 is f = 1.2 and there is significant pulse narrowing. This narrowing is typical of the detuning range between f = 3 and f = 1.2. As the detuning decreases to f = 1.1 or lower, a significant fraction of the input pulse is reflected from the grating and the intensity in the grating is significantly reduced for smaller detunings. This reduced intensity decreases the nonlinear interactions and the pulse width increases, first back to its initial width and then it broadens for even smaller detunings due to the strong grating dispersion.

We find that the threshold for the polarization instability decreases as the pulse wavelength is tuned toward the short wavelength edge of the photonic bandgap. For detunings near f = 1.3 the threshold is reduced by approximately a factor of three relative to the threshold for detunings larger than f = 4, where the threshold is nearly equal to that predicted for fiber with the grating birefringence but no enhancement in nonlinearity or birefringence. This decreased threshold for wavelengths near the gap is in agreement with our numerical models. It is also consistent with the enhancement of the effective nonlinearity given by Eq. (3) and the relative insensitivity of the birefringence for tuning close to the gap. Our numerical modeling also shows that this enhancement depends on asymmetry of the X and Y gaps shown in Figure 1. For symmetric X and Y gap widths the simulations predict that the enhancement is significantly less.

For longer pulse lengths with correspondingly narrower frequency spreads, the simulations show that over an order of magnitude decrease in the polarization instability threshold can be achieved. These large decreases in the threshold are a result of being able to tune very close to the bandgap edge and still avoid reflection from the grating when the pulse frequency spread is very small.

At the long wavelength edge of the gap, normal dispersion, combined with the nonlinear interaction, results in pulse broadening as the intensity is increased to the nonlinear regime[1]. The birefringence is larger at the long wavelength gap edge because of the asymmetry in the fast and slow gap widths for our experimental parameters. The net result of these differences between the short and long wavelength edges of the gap is that the threshold intensity for the polarization instability increases as the pulse wavelength is tuned near the long wavelength gap edge.

In our experiments the effective birefringence and grating length correspond to less than a polarization beat period, i.e.

$$2\pi L(n_y - n_x)/\lambda_o \sim \pi/2 \qquad (7)$$

where L is the grating length. The optimum length for the polarization instability is near one beat period[2,3].

For applications it is interesting that the intensity, corresponding to the input energy, required to switch a significant fraction of the pulse energy from the fast to the slow axis can be made very low by tailoring the grating birefringence to be small. Of course, when the birefringence is decreased, the grating must be made correspondingly longer in order to obtain a beat length in the grating. A practical optical switching device based of this effect would require switching energies in the picojoule regime instead of the hundreds of nanojoules used in the present experiments. Optical switching will probably be interesting for pulse widths near one picosecond and wavelengths near 1.5 microns. The wide pulse spectrum of a picosecond pulse would require a correspondingly wider grating gap width near 10 nm. Larger gap widths and much larger nonlinear coefficients can be obtained using a combination of waveguide geometries and materials with much larger nonlinear coefficients than silica fiber. Examples of materials with nonlinearities at least 500 times that of silica glass at 1.5 micron wavelengths are AlGaAs, chalcogenide glasses and cascaded second-order nonlinearities in $LiNbO_3$. All of these materials can be formed into waveguides at least a few centimeters in length with relatively low linear losses. Gratings with large index modulation can be lithographically etched into these waveguides. Birefringence in the waveguide gratings should be relatively simple to design for specific values. Since the waveguide mode areas can be significantly less than those in optical

fiber, the required intensity for optical switching with picojoule energy inputs seems to be within reach. The nonlinear losses in these materials are also reasonably low for optical switching applications.

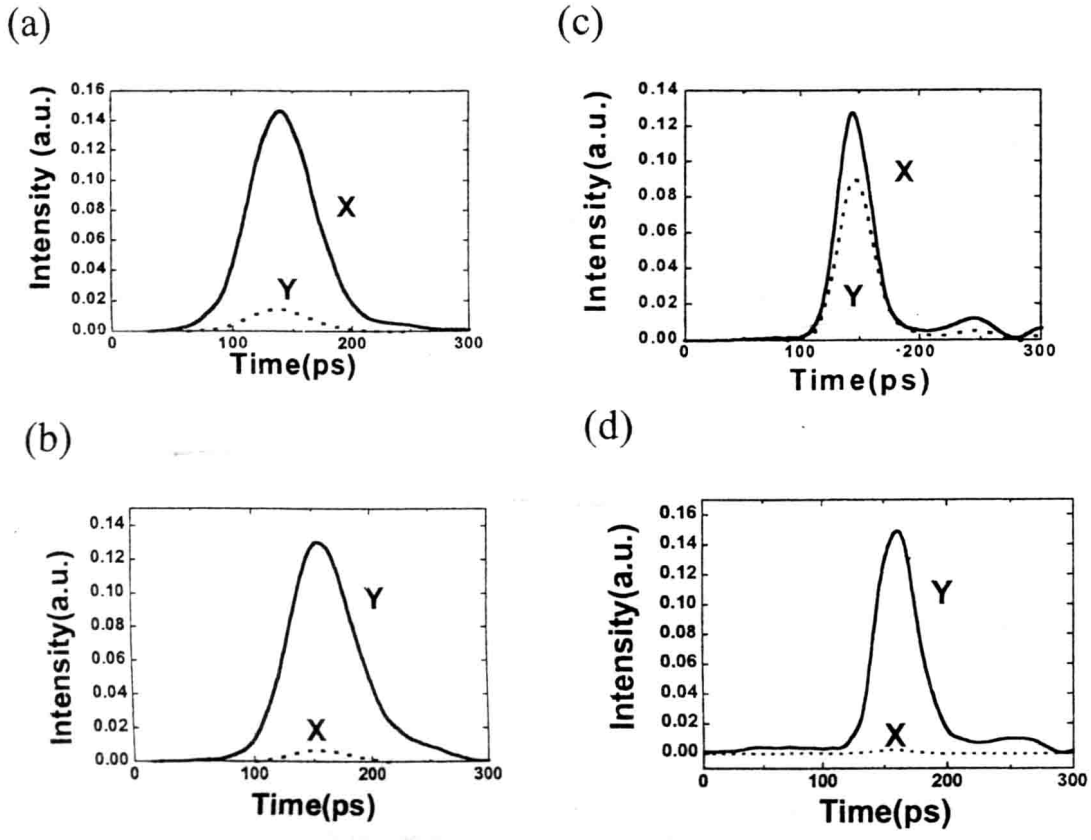

Figure 4 Pulse shapes for the X and Y polarization components transmitted in the linear regime are shown for the polarization predominantly along the fast X axis (a) and predominantly along the slow Y axis (b). The nonlinearly transmitted pulse shapes corresponding to (a) and (b) are shown in (c) and (d) respectively. The peak pulse intensity in (c) and (d) is approximately 4 GW/cm^2 along each axis. The detuning in all cases is f = 1.2. The fast and slow components are in phase at the input face of the fiber.

4. VECTOR BRAGG SOLITONS

When the detuning is near f = 1.1 and the polarization is aligned exactly along one of the principle axes, the lowest order Bragg soliton can be generated at peak pulse intensities near 10 GW/cm^2. The Bragg soliton formation length is approximately[1]

$$z_o = 0.322\pi\tau_e^2/2\,|\beta_2| \qquad (7)$$

where τ_e is the pulse width of the emerging soliton. For τ_e = 80ps and a detuning value near f = 1.2, this formation length is near 2 cm. Our grating length of 6 cm does not allow full evolution into a soliton, but the formation length is much less than

in fiber without a grating. A study of the soliton formation process is certainly possible for our experimental grating parameters.

It is very interesting that for our grating parameters the polarization instability dominates the pulse dynamics unless the polarization is very near the slow axis or exactly along the fast axis. The polarization instability threshold intensity tends to be lower than the Bragg soliton formation intensity. Since the birefringence can be adjusted by the grating fabrication process, this means that the threshold for the polarization instability can be set relative to the threshold for Bragg soliton formation along the fast or slow axis.

Soliton formation for the general vector case of both fast and slow polarization components has been studied for the normal fiber case both theoretically[7] and experimentally[8]. The energy exchange between the fast and slow components varies with the relative phase between the fast and slow components as can be seen from the energy exchange terms in Eqs. (5) and (6). For example, for a phase shift between the fast and slow components of $\pi/2$ and a given angle between the fast and slow components we expect a soliton to evolve from the coupled nonlinear Schröedinger equations for a specific input pulse shape and energy. Experiments and numerical modeling are in progress for the study of vector Bragg solitons.

ACKNOWLEDGEMENTS

The authors thank Tom Strasser for his guidance on the design and fabrication of the fiber gratings used in these experiments. This work was supported in part by the Natural Sciences and Engineering Research Council of Canada (NSERC).

REFERENCES

1. B.J. Eggleton, C. Martijn de Sterke and R. E. Slusher, "Bragg soitons in the nonlinear Schroedinger limit: experiment and theory," *J. Opt. Soc. Am. B*, **16**, pp. 587-599, 1999.
2. H.G. Winful, "Self-induced polarization changes in birefringent optical fibers," *Applied Phys. Lett.*, **47**, pp. 213-215, 1985.
3. H. G. Winful, " Polarization instabilities in birefringent nonliear media: application to fiber-optic devices," *Optics Letters*, **11**, pp.33-35, 1986.
4. S. Trillo, S. Wabnitz, R. H. Stolen, G. Assanto, C. T. Seaton, and I. Stegeman, "Experimental observation of polarization instability in a birefringent optical fiber," *Appl. Phys. Lett.* **49**, pp. 1224-1226, 1986.
5. Suresh Pereira and J. E. Sipe, "Nonlinear pulse propagation in birefringent fiber Bragg gratings," *Optics Express* **3**, pp. 418-432, 1998.
6. D.Taverner, N. G. R. Broderick, D. J. Richardson, M. Ibsen, R. I. Laming, "All-optical "AND" gate based on coupled gap soliton formation in a fibre Bragg grating," *Optics Lett.* **23**, pp. 259-261, 1998.
7. Nail Akhmediev, Alexander Buryak, and J. M. Soto-Crespo, "Elliptically polarized solitons in birefringent optical fibers," *Opt. Comm.*, **112**, pp. 278-282, 1994.
8. Y. Barad and Y. Silberberg, "Polarization evolution and polarization instability of solitons in a birefringent optical fiber," *Phys. Rev.Lett.*, 78, pp. 3290-3293, 1997.

Invited Paper

Multi-wavelength and multi-colour temporal and spatial optical solitons

Yuri S. Kivshar[a], Andrey A. Sukhorukov[a], Elena A. Ostrovskaya[a], Ole Bang[a,b], and Carl Balslev Clausen[b]

[a] Optical Sciences Centre, Research School of Physical Sciences and Engineering
Australian National University, Canberra, Australia
[b] Department of Mathematical Modelling, Technical University of Denmark
Lyngby DK-2800, Denmark

ABSTRACT

We present an overview of several novel types of multi-component envelope solitary waves that appear in fiber and waveguide nonlinear optics. In particular, we describe multi-channel solitary waves in bit-parallel-wavelength fiber transmission systems for high performance computer networks, multi-colour parametric spatial solitary waves due to cascaded nonlinearities of quadratic materials, and quasiperiodic envelope solitons in Fibonacci optical superlattices.

Keywords: Envelope optical solitons, cascaded nonlinearities, multistep cascading, bit-parallel-wavelength transmission systems, Fibonacci superlattices

1. INTRODUCTION

Recent progress in the design and manufacture of optical fiber wavelength-division-multiplexing (WDM) systems is a result of worldwide demand for ultra-high bit-rate transmission and communication. This explains the growing interest from the soliton community to study the pulse propagation in the soliton-based optical fiber communication systems, and remarkable progress has been demonstrated in recent years.[1] On one hand, the recent results include the application of the concept of the dispersion management to soliton-based optical transmission systems and the discovery of the so-called *dispersion managed soliton*. On the other hand, this progress involves the development of *completely new concepts* for pulse dense packing and increased bit-rate per channel techniques. One such new concept is the bit-parallel-wavelength pulse transmission for very high bandwidth computer communications that offers many of the advantages of both parallel fiber ribbon cable and conventional WDM systems.[2]

Rapid progress in the study of temporal solitons in fiber systems has been observed in parallel with impressive research on their spatial counterparts, *spatial optical solitons*. One of the key concepts in this field came from the theory of multi-frequency wave mixing and cascaded nonlinearities where a nonlinear phase shift is produced as a result of the parametric wave interaction.[3] In all such systems, the nonlinear interaction between the waves of two (or more) frequencies is the major physical effect that supports coupled-mode solitary waves.

The main purpose of this contribution is to overview several different physical examples of multi-mode and/or multi-frequency solitary waves that occur in the pulse or beam propagation in nonlinear optical fibers and waveguides. For these purposes, we select *three different, but physically interesting cases*, multi-wavelength solitary waves in bit-parallel-wavelength optical fiber links, multi-colour spatial solitons due to multistep cascading in optical waveguides with quadratic nonlinearities, and quasiperiodic solitons in the Fibonacci superlattices. We believe these examples display both the diversity and richness of the multi-mode soliton systems, and they will allow further progress to be made in the study of nonlinear waves in multi-component nonintegrable physical models.

Yuri Kivshar's e-mail: ysk124@rsphysse.anu.edu.au

In *Optical Pulse and Beam Propagation II*, Yehuda B. Band, Editor,
Proceedings of SPIE Vol. 3927 (2000) • 0277-786X/00/$15.00